This is the peer reviewd version of the followng article:

Multi three-phase hairpin windings for high-speed electrical machine: Possible implementations / Pastura, M.; Barater, D.; Nuzzo, S.; Franceschini, G.. - (2021), pp. 113-118. (Intervento presentato al convegno 2021 IEEE Workshop on Electrical Machines Design, Control and Diagnosis, WEMDCD 2021 tenutosi a ita nel 2021) [10.1109/WEMDCD51469.2021.9425640].

Institute of Electrical and Electronics Engineers Inc.
Terms of use:

The terms and conditions for the reuse of this version of the manuscript are specified in the publishing policy. For all terms of use and more information see the publisher's website.

23/04/2024 17:05

(Article begins on next page)

Multi Three-Phase Hairpin Windings for High-Speed Electrical Machine: Possible Implementations

Marco Pastura
Dept. of Engineering Enzo Ferrari
University of Modena and Reggio
Modena, Italy
marco.pastura@unimore.it

Davide Barater
Dept. of Engineering Enzo Ferrari
Università di Modena e Reggio Emilia
Modena, Italy
davide.barater@unimore.it

Stefano Nuzzo
Dept. of Engineering Enzo Ferrari
Università di Modena e Reggio Emilia
Modena, Italy
stefano.nuzzo@unimore.it

Giovanni Franceschini
Dept. of Engineering Enzo Ferrari
Università di Modena e Reggio Emilia
Modena, Italy
giovanni.franceschini@unimore.it

***Abstract*—This work provides an in-depth critical analysis related to the feasibility of combining multi three-phase winding layouts with the ever-spreading hairpin technology. After an introduction on the advantages and challenges of both hairpin and multi-phase windings, more details on how these two technologies can be combined are provided. Then two similar stator geometries, with 72 and 96 slots, are analyzed in detail exploiting an 8 poles permanent magnet – assisted synchronous reluctance motor for traction applications. A relevant set of feasible winding configurations are modelled and analyzed through finite element simulations. For every machine, a breakdown of the power losses is provided and compared against that of the same machine topologies having random-wound windings with stranded round conductors. The main results and possible solutions to increase the machine performance are then provided.**

Keywords—AC losses, Automotive, Hairpin, High-Speed, Multi three-phase, Multi-phase

I. INTRODUCTION

In the last decade, the research interest for both hybrid and full electric vehicles (EVs) has grown due to the need of decreasing the greenhouse gas emissions [1]. EVs for the automotive sector require high performance, which mostly consists in achieving high torque values in the low-to-mid speed range, while reaching high speeds through a wide flux weakening capability. In addition, in the perspective of a larger scale production, cost reduction and faster automated manufacturing processes need to be considered as design objectives. The electric automotive sector demands for high speed and high torque density solutions have led to electrical machines equipped with bar-wound conductors, such as hairpins. However, other solutions can be considered as performance improvement methodologies, such as winding topologies different from the conventional three-phase (3-phase) ones.

A. Hairpin Windings

Hairpin windings are made of pre-formed conductors which can achieve higher fill factors compared to standard random-wound windings, thus resulting in a higher torque density [2], [3]. The increase of the amount of copper in the slot with respect to the insulation material determines a greater thermal conductivity, thus improving the cooling capability [4]. In addition, they are more suitable for an automated winding process [5], so the overall stator cost can be decreased as proved in [6]. However, there are also some challenges associated to hairpin conductors. In automotive applications the operating frequency can reach values above 1 *kHz*, determining high AC losses [7]-[11]. AC losses in hairpin conductors are mostly due to skin and proximity effects mainly caused by the leakage flux produced by the stator currents. These phenomena make the current distribution within the hairpins ununiform and, additionally, each conductor within the same slot features its own distribution, with the worst scenarios occurring on the closest conductors to the airgap. Hence, Joule losses are not evenly distributed inside the slot but are accentuated near the airgap where there is a larger influence of leakage fluxes [7]. In conclusion, at high frequency operations, the overall efficiency tends to decrease. Some practical solutions have been proposed to reduce AC losses. These include:

1) decreasing the total amount of copper in the slot and pushing the conductors towards the slot bottom, thus increasing the distance from the slot opening [7]. However, this solution results in a lower fill factor, which is one of the main benefits of hairpin windings;
2) increasing the number of conductors, whose effectiveness depends on the frequency range. However, a higher number of conductors increases the manufacturing complexity and slightly decreases the fill factor [3];
3) adopting new winding concepts, such as segmented [8] or asymmetric [9] bar layouts. However, also these solutions increase the manufacturing complexity. Another possibility is to use a higher resistivity material for the conductors near the airgap, as proposed in [12].

A good trade-off is represented by the method described in 2), which is then the most used way to overcome the inherent elevated AC losses associated to hairpin windings at high frequencies.

B. Multi 3-phase machines

Using bar-wound conductors is not the only way to meet the torque density requirements demanded nowadays by automotive applications. To such purposes, multi-phase machines can be a suitable solution. Basically, these are electrical machines with a number of phases $m > 3$. Usually

XXX-X-XXXX-XXXX-X/XX/$XX.00 ©20XX IEEE

m is five, seven or a multiple of three [13]. The latter case often refers to the so called multi 3-phase machines, where the stator winding layout is composed by *m/3* separated star-connected 3-phase windings. These machines are of great interest thanks to their modularity. Being composed by a certain number of 3-phase winding sets, they can be fed by the same number of 3-phase voltage source inverters (VSIs), avoiding the need of a specific *m*-phase power converter. The main characteristics of multi 3-phase machines are:

- Higher fundamental winding factor, which determines a higher torque density [14]-[16].
- Lower spatial harmonic content, which results in lower rotor losses and reduced torque ripple [14], [15], [17].
- Higher reliability, due to the inherent fault tolerant capability [14], [15], [18].
- Possibility of decreasing the converter power rating thanks to the splitting of the feeding current in more than three phases [15]-[17].
- Lower turns per phase, which determines a lower leakage inductance thus leading to higher undesirable harmonic currents and additional Joule losses, in particular when VSIs with a standard PWM are employed [17].
- More complex control strategies due to the higher number of converters and the mutual couplings between the different 3-phase sets. In addition, the mutual couplings and the lower leakage inductances can trigger dangerous harmonic currents. These drawbacks can be, at least partially, overcome with a proper control strategy [19].

C. Aim of the study

Basing on the above considerations, the combination of the two described technologies, i.e. hairpin and multi 3-phase windings, could represent an interesting solution for the development of high-performance electric machines for automotive applications.

The aim of the paper is then to investigate and provide a critical analysis on the combined use of multi 3-phase windings and hairpin conductors, illustrating main advantages and drawbacks. Starting from some performance requirements for an automotive application, different solutions are provided and compared through finite element (FE) electromagnetic analyses.

II. Case Study

As vehicle to investigate multi 3-phase hairpin windings in traction motors, a permanent magnet – assisted synchronous reluctance machine is considered. Keeping the initial rotor design, i.e. an 8 poles rotor, and the main stator dimensions unaltered, two slot combinations are studied, i.e. 72 and 96 slots. A summary of the main machine parameters and requirements is provided in Table I.

Considering the limits of applicability of hairpin windings, the focus is on the different multi 3-phase hairpin structures which can be adopted for both configurations. For each hairpin winding arrangement, all the simulation results are compared to their random-wound counterparts equipping stranded round conductors. In terms of modelling assumptions, the main differences between bar- and random-wound solutions are:

TABLE I. Machine Main Parameters and Requirements

Machine Type	
PM-Assisted (NdFeB) SynRel	
Slot Combinations	
72	96
Rotor Poles	
8	
Speed [rpm]	***Torque [N.m]***
5000 (Base)	400
15000 (Max)	140
DC Link Bus Voltage [V]	
620	

- The fill factor is assumed equal to 40% for the random arrangement, whereas an 80% fill factor is considered for the hairpin winding.
- AC losses are considered null for the random-wound windings, inherently meaning that each conductor comprises a high number of parallel strands which make the current distribution uniform within the considered frequency range. On the other hand, each hairpin leg is modelled as solid conductor using a suitable mesh density. This allows to take all the AC losses components into account.

A. Feasibility Analysis

When designing an electrical machine for high-speed applications, the number of turns and parallel paths have to be carefully chosen to remain within the voltage limits. While for classical stranded conductors the number of degrees of freedom is quite high, more constraints are in place for machines with hairpin conductors. In [10] and [11], some important guidelines are provided for the realization of hairpin windings, with a particular focus on the maximum number of parallel paths which allows a correct conductors' transposition. Only integral slot distributed windings are considered (ISDW) in those works. As reported in [10], the minimum number of series connected turns N_{sct} can be determined as in (1), while the maximum number of parallel paths n_{pp} which allows a correct transposition and uniform connections is calculated using (2). *LCM* means least common multiple, n_w is the number of hairpin conductors per slot, p is the number of poles and q is the number of slots-per-pole-per-phase. The examples shown in [10] and [11] refer to 3-phase windings, however all the assumptions and considerations can be extended to multi 3-phase configurations. In fact, considering a balanced multi 3-phase ISDW, each 3-phase set is equally and evenly distributed along the stator circumference. The number of slots-per-pole-per-phase is lower but remains an integer. Hence, all the rules provided in [10] and [11], as well as the expressions reported in (1) and (2), can be applied separately to each 3-phase set.

$$N_{sct} = LCM\left\{\frac{n_w p}{4}, q\right\} \quad (1)$$

$$n_{pp} = \frac{pqn_w}{2N_{sct}} \quad (2)$$

Considering the 72 slots solution, in order to meet both the required performance and the voltage limit, for the 3-phase machine n_w is chosen equal to 6, while $n_{pp} = 4$. According to (2), n_{pp} could be higher, but increasing the number of paths would increase the manufacturing complexity. A higher n_w could result in reduced AC losses, but it would not be applicable due to the voltage limit. In fact, when $n_w = 8$ or 10,

TABLE II. COMPARISON BETWEEN 3- AND 9-PHASE TOPOLOGIES FOR 72 STATOR SLOTS WITH HAIRPIN AND STRANDED ROUND CONDUCTORS

	Hairpin		*Random*	
Parameter	***3-phase***	***9-phase***	***3-phase***	***9-phase***
q	3	1	3	1
n_w	6	6	6	6
n_{pp}	4	2	4	2
N_t	18	12	18	12
Line Current $[A_{rms}]$	454.68	227.34	454.68	227.34
Number of Converters	1	3	1	3
Winding Factor	0.96	1	0.96	1

TABLE III. COMPARISON BETWEEN 3-, 6- AND 12-PHASE TOPOLOGIES FOR 96 STATOR SLOTS WITH HAIRPIN CONDUCTORS

	3-phase	***6-phase***	***12-phase***
q	4	2	1
n_w	6	6	6
n_{pp}	8	4	2
N_t	12	12	12
Line Current (A_{rms})	682	341	170.5
Number of converters	1	2	4
Winding Factor	0.957	0.99	1

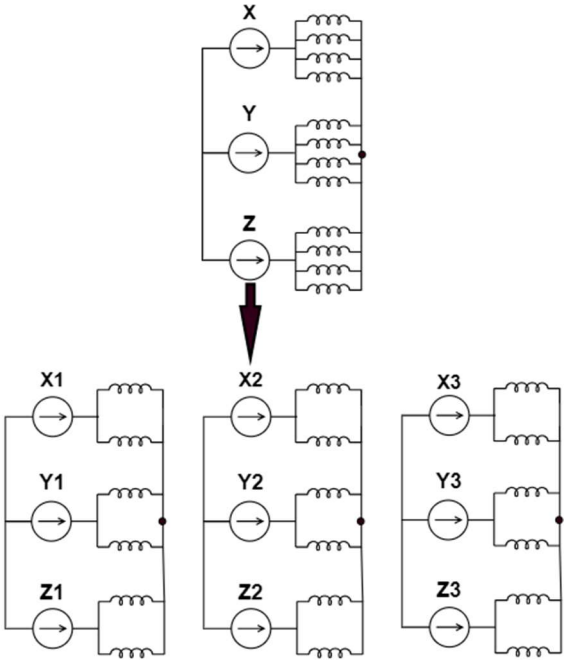

Fig. 1. Winding layouts examples for the 72 slots stator. Transformation of a 3-phase winding with 3 slots-per-pole-per-phase and 4 parallel paths per phase into a triple 3-phase configuration with 1 slot-per-pole-phase and 2 parallel paths per phase.

n_{pp} is limited to 2. However, the 72 slots, 8 poles 3-phase winding can be converted only into a 9-phase one with three 3-phase sets having an electrical shift of 20°. The 6- and 12-phase solutions would not be feasible for the 72 slots configuration since q would no longer be an integer like in the 3-phase winding. With $n_{pp} = 2$, the number of series-connected turns of each phase is multiplied by 2/3 (if the same n_w is adopted), allowing a lower phase voltage although the number of parallel paths per phase is halved. Fig. 1 shows how to pass from a 3- to a 9-phase winding halving n_{pp}. On the other hand, always taking into account the manufacturing aspects, it could be also possible to rise n_w to 8 without exceeding the voltage constraints. A higher number of n_w would also allow for a lower phase current if the power was kept constant, so lower Joule losses would be expected. Table II resumes the main differences between the 3- and 9-phase windings. N_t represents the number of series-connected turns for each parallel path of any phase. The winding factor refers to the fundamental harmonic, therefore the 9-phase machine is expected to have a higher torque. Here the 9-phase machine with $n_w = 6$ and $n_{pp} = 2$ is investigated since it can provide a better exploitation of the torque-speed characteristic. However, also the case with $n_w = 8$ is reported for the sake of comparison in terms of Joule losses.

In order to study a different number of 3-phase sets, the 96 slots configuration is exploited, where 6- and 12-phase winding arrangements are possible in addition to the conventional 3-phase one. If $n_w = 6$, the 3-phase solution would require 8 parallel paths per phase which could provide some challenges with respect to the end winding connections and conductors' transpositions. Therefore, the analysis on the 96 slots, 3-phase machine will not be provided. Transforming the 3-phase winding either into a 6- or a 12-phase layout permits reducing the number of parallel connections per phase to 4 or 2 respectively, without exceeding the voltage constraints. Table III summarises the main parameters of the possible solutions. The data for the random windings with stranded conductors are omitted in Table III since they are basically the same as the hairpin machines.

The windings with round, stranded conductors have fewer constraints in terms of conductors per slot and parallel paths. Therefore, to simplify and making the comparison fully fair, 6 equivalent stranded conductors per slot are considered for all the winding configurations.

III. FINITE ELEMENT ANALYSIS

A. General considerations and parameters estimation

All the described machine topologies are analysed through FE models. All of these models implement the same identical materials for cores, windings and magnets. For a fixed slot number, the only difference from a 3-phase machine and its multi 3-phase counterpart consists in the winding arrangement so that the comparison can be easier and fairer. As the overall stator dimensions are kept unmodified when passing from random to hairpin windings, the latter features a higher amount of copper than random layouts, due to their higher fill factor.

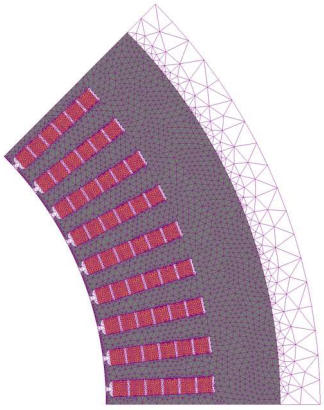

Fig. 2. 72 slots solid conductor 2D stator model with $n_w = 6$. The initial mesh is displayed.

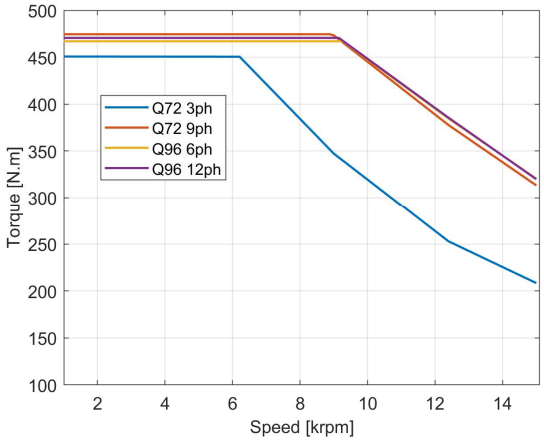

Fig. 3. Torque vs speed characteristic approximation for the different hairpin winding machines. Q refers to the number of slots.

TABLE IV. SIMULATION RESULTS FOR THE 72 SLOT MODELS AT 5000 RPM

Simulation at 5 krpm	*3-phase*		*9-phase*	
	Hairpin	**Round**	**Hairpin**	**Random**
Torque [Nm]	451	452	475	477
Active Winding Losses [W]	4044	2361	4156	2361
End Winding Losses [W]	1194	2386	1194	2386
Total Winding Losses [W]	5238	4747	5350	4747
Magnet Joule Losses [W]	17.8	18.4	9.7	9.8
Rotor Iron Losses [W]	237	237	218	220
Stator Iron Losses [W]	2790	2730	2851	2780
Total Losses [W]	8283	7732	8428	7757
Efficiency [%]	96.6	96.8	96.7	97

The FE simulations are performed using MagNet software and exploiting its 2D modelling features, meaning that the end windings are neglected and the border effects cannot be computed. However, the DC component of the end winding losses can be calculated for all the cases using (3) for the estimation of the end winding length l_{ew} [20]. In (3), c_s is the average coil span. In [20], (3) is proposed for random windings, while front and back connections of hairpin conductors are typically shorter.

$$l_{ew} = 2.4c_s + 0.1\ [m] \qquad (3)$$

In addition, always concerning the end winding losses, the effective value depends on the ratio R_{ac}/R_{dc} between AC and DC resistances. In the end region, the field strength is much lower than in the core, so the ratio R_{ac}/R_{dc} can be near to the unit depending on the machine geometries. If the flux density is sufficiently low, the ratio R_{ac}/R_{dc} would be near to 1 even at high operating frequencies (e.g. at ≈ 1 kHz), so an approximation of the end winding losses as purely DC would be acceptable. A 3D analysis of the end winding AC losses is provided in [21] for a single coil. The R_{ac}/R_{dc} ratio in the end windings tends to increase much slower compared to that of the active part of the machine and its value is influenced also by saturation and temperature. More precisely, higher

TABLE V. SIMULATION RESULTS FOR THE 96 SLOT MODELS AT 5000 RPM

Simulation at 5 krpm	*6-phase*		*12-phase*	
	Hairpin	**Round**	**Hairpin**	**Random**
Torque [N.m]	466	467	471	472
Active Winding Losses [W]	2995	3987	3000	3987
End Winding Losses [W]	1986	3973	1986	3973
Total Winding Losses [W]	4980	7960	4986	7960
Magnet Joule Losses [W]	6.3	6.0	6.2	5.9
Rotor Iron Losses [W]	151	157	149	156
Stator Iron Losses [W]	2253	2216	2267	2230
Total Losses [W]	7390	10339	7408	10352
Efficiency [%]	97	95.9	97	95.9

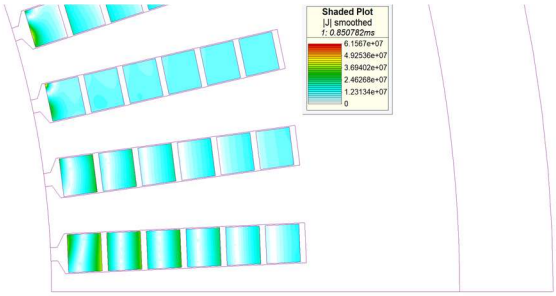

Fig. 4. Instantaneous current density at base speed for the 72 slots machine.

temperature and saturations tend to lower the ratio in favour of a higher DC component, especially for a few hundreds of Hz. Although the R_{ac}/R_{dc} ratio in the end windings is assumed equal to 1 in this paper, further research is needed to investigate the high-frequency behaviour of hairpin windings in the end regions.

B. Simulations and results

All the studied machines (see Tables II and III) are modelled exploiting their periodicities. For both the 72 and 96 slots models, having both an 8 poles ISDW, there is a 1/8 odd periodicity, so 1/8 of each machine is analyzed as shown in Fig. 2, where the modelled angular sector of the 72 slots stator can be observed together with the mesh used.

The simulations are run using sinusoidal current sources feeding the stator phases. The torque-speed charts of each machine are estimated through the simulation at some relevant operating frequencies assuming a continuous power operation. All the results consider the fundamental harmonic voltage limit provided by a space vector pulse width modulation (SVPWM) scheme having a DC link voltage of 620 V. The value is computed through an FFT analysis of the induced voltages across the machine coils when the machine rated current is applied. Fig. 3 shows the estimated torque-speed characteristics for the hairpin winding machines. The 9-phase machine has a higher torque with respect to the 3-phase case and permits extending the constant torque region thanks to the lower number of series-connected turns per phase. The 6- and 12-phase configurations for the 96 slots machines have very similar curves and torques. In fact, they feature almost the same fundamental winding factor and the same number of series-connected turns per phase. The main

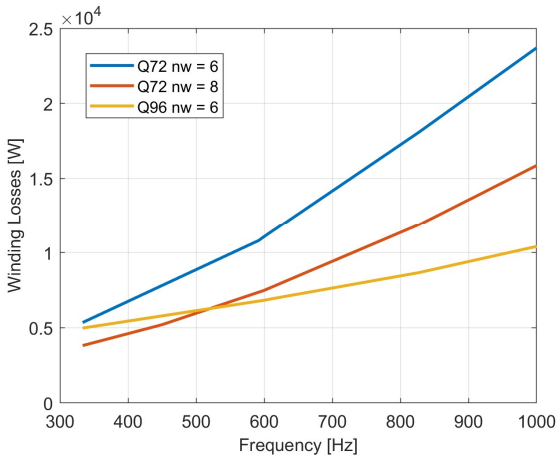

Fig. 5. Winding losses as function of frequency for different conductor number used in the analyzed machines.

difference consists in the higher number of parallel paths for the 6-phase configuration, so more attention is needed for the conductors' transpositions. For all the machines having parallel paths particular attention should be given to the transposition methods, which need to be carried out in such a way that all the parallel connections have the same overall impedance, as explained in [10] and [11].

Table IV and Table V provide a summary in terms of losses for all the analyzed machines at the base speed of 5000 rpm, also highlighting the comparison against the same machines equipped with random windings. Considering the active windings, the relevant losses in the 72 slots machines equipped with hairpins are higher than those in machines with random windings. This is an expected result as AC losses are present in the hairpin conductors at base speed already, as seen from the current density map shown in Fig. 4. For the 96 slots machines, at base speed, the active windings Joule losses are lower for the solid conductors compared to the stranded round ones, contrarily to what happens with the 72 slots case. This means that in the 96 slots machine the winding has a lower R_{ac}/R_{dc} ratio than the 72 slots case study. The lower ratio is caused by the smaller hairpin dimensions. However, including the DC component of the end winding losses, the total losses for the solid conductors result more similar to those of the stranded round ones for the 72 slots winding, while they are fairly lower for the 96 slots one. Basing on the considerations made in section III.A, the DC component at the speed of 5000 rpm (333.33 Hz) is predominant in the end region, so the contribution of the end winding losses is in favor of the hairpin winding. However, at higher operating frequencies, the Joule losses in hairpin conductors significantly increase and are more elevated than in the corresponding random winding machines, even considering the DC loss component of the end winding. The strong frequency dependence of the solid conductors' Joule losses can be seen in Fig. 5. Fig. 5 shows the total winding losses as a function of frequency for the different stator topologies with hairpins. The lower R_{ac}/R_{dc} ratio determines a flatter loss curve for the 96 slots machine, while an improvement for the 72 slots machine winding losses can be achieved if $n_w = 8$ (feasible only with a 9-phase layout) is adopted. Regarding the efficiency, the adoption of multi 3-phase windings does not provide a significant improvement at base speed, while it can provide a good increment at the higher speeds thanks to the wider constant torque speed region (Fig. 3) which allows a higher output power.

IV. Conclusion

This work has addressed the possibility of adopting multi 3-phase windings with hairpin conductors for high torque, high speed electrical machines for traction applications. The main aspects which have been underlined are as follows:

- The possibility of achieving a higher torque thanks to a higher fundamental winding factor.
- The possibility of increasing the number of conductors per slot, compatibly with manufacturing aspects, without exceeding the voltage limits.
- The possibility of obtaining a wider constant torque speed region thanks to the lower number of phase series-connected turns.
- The possibility of reducing the number of parallel paths maintaining nearly the same performance or even increasing it.
- The importance of considering the end winding losses when a choice has to be done between a classical winding with stranded round conductors and a hairpin technology. The study of the AC losses in solid conductors has always been focused on the active parts. However, the end winding loss component can be significant and there is a lack of research on the influence of AC losses in this part of the machine for hairpin conductors.

V. Acknowledgment

This project has received funding from the Clean Sky 2 Joint Undertaking under the European Union's Horizon 2020 research and innovation programme under project AUTO-MEA grant agreement No. 865354.

References

[1] R. T. M. Smokers, M. Verbeek and S. van Zyl, "EVs and post 2020 CO2 targets for passenger cars," *2013 World Electric Vehicle Symposium and Exhibition (EVS27)*, Barcelona, 2013, pp. 1-11, doi: 10.1109/EVS.2013.6915006.

[2] Y. Zhao, D. Li, T. Pei and R. Qu, "Overview of the rectangular wire windings AC electrical machine," in *CES Transactions on Electrical Machines and Systems*, vol. 3, no. 2, pp. 160-169, June 2019, doi: 10.30941/CESTEMS.2019.00022.

[3] A. Arzillo *et al*., "Challenges and Future opportunities of Hairpin Technologies," *2020 IEEE 29th International Symposium on Industrial Electronics (ISIE)*, Delft, Netherlands, 2020, pp. 277-282, doi: 10.1109/ISIE45063.2020.9152417.

[4] A. Reinap, M. Andersson, F. J. Márquez-Fernández, P. Abrahamsson and M. Alaküla, "Performance Estimation of a Traction Machine with Direct Cooled Hairpin Winding," 2019 IEEE Transportation Electrification Conference and Expo (ITEC), Detroit, MI, USA, 2019, pp. 1-6, doi: 10.1109/ITEC.2019.8790545.

[5] F. Wirth, T. Kirgör, J. Hofmann and J. Fleischer, "FE-Based Simulation of Hairpin Shaping Processes for Traction Drives," *2018*

8th International Electric Drives Production Conference (EDPC), Schweinfurt, Germany, 2018, pp. 1-5, doi: 10.1109/EDPC.2018.8658278.

[6] C. Du-Bar, A. Mann, O. Wallmark and M. Werke, "Comparison of Performance and Manufacturing Aspects of an Insert Winding and a Hairpin Winding for an Automotive Machine Application," 2018 8th International Electric Drives Production Conference (EDPC), Schweinfurt, Germany, 2018, pp. 1-8.

[7] C. Du-Bar and O. Wallmark, "Eddy Current Losses in a Hairpin Winding for an Automotive Application," 2018 XIII International Conference on Electrical Machines (ICEM), Alexandroupoli, 2018, pp. 710-716, doi: 10.1109/ICELMACH.2018.8507265.

[8] A. Arzillo et al., "An Analytical Approach for the Design of Innovative Hairpin Winding Layouts," 2020 International Conference on Electrical Machines (ICEM), Gothenburg, 2020, pp. 1534-1539, doi: 10.1109/ICEM49940.2020.9270927.

[9] M. S. Islam, I. Husain, A. Ahmed and A. Sathyan, "Asymmetric Bar Winding for High-Speed Traction Electric Machines," in IEEE Transactions on Transportation Electrification, vol. 6, no. 1, pp. 3-15, March 2020.

[10] G. Berardi, N. Bianchi, "Design guideline of an AC hairpin winding", 2018 XIII International Conference on Electrical Machines (ICEM), pp. 2444-2450, 3.-6. Sept. 2018.

[11] N. Bianchi and G. Berardi, "Analytical Approach to Design Hairpin Windings in High Performance Electric Vehicle Motors," 2018 IEEE Energy Conversion Congress and Exposition (ECCE), Portland, OR, 2018, pp. 4398-4405.

[12] X. Fan, D. Li, R. Qu, C. Wang and J. Li, "Hybrid Rectangular Bar Wave Windings to Minimize Winding Losses of Permanent Magnet Machines for EV/HEVs over a Driving Cycle.," *2018 IEEE International Magnetics Conference (INTERMAG)*, Singapore, 2018, pp. 1-2, doi: 10.1109/INTMAG.2018.8508038.

[13] A. Hebala et al., "Feasibility Design Study of High-Performance, High-Power-Density Propulsion Motor for Middle-Range Electric Aircraft," 2020 IEEE 29th International Symposium on Industrial Electronics (ISIE), Delft, Netherlands, 2020, pp. 300-306, doi: 10.1109/ISIE45063.2020.9152551.

[14] F. Barrero and M. J. Duran, "Recent Advances in the Design, Modeling, and Control of Multiphase Machines—Part I," in IEEE Transactions on Industrial Electronics, vol. 63, no. 1, pp. 449-458, Jan. 2016.

[15] E. Levi, "Multiphase Electric Machines for Variable-Speed Applications," in *IEEE Transactions on Industrial Electronics*, vol. 55, no. 5, pp. 1893-1909, May 2008.

[16] Y. Burkhardt, A. Spagnolo, P. Lucas, M. Zavesky and P. Brockerhoff, "Design and analysis of a highly integrated 9-phase drivetrain for EV applications," *2014 International Conference on Electrical Machines (ICEM)*, Berlin, 2014, pp. 450-456.

[17] M. Diana, R. Ruffo and P. Guglielmi, "Low torque ripple tooth coil windings multi-3-phase machines: design considerations and validation," in IET Electric Power Applications, vol. 14, no. 2, pp. 262-273, 2 2020.

[18] P. Giangrande, V. Madonna, S. Nuzzo, C. Gerada and M. Galea, "Braking Torque Compensation Strategy and Thermal Behavior of a Dual Three-Phase Winding PMSM During Short-Circuit Fault," 2019 IEEE International Electric Machines & Drives Conference (IEMDC), San Diego, CA, USA, 2019, pp. 2245-2250, doi: 10.1109/IEMDC.2019.8785164.

[19] J. Karttunen, S. Kallio, P. Peltoniemi, P. Silventoinen and O. Pyrhönen, "Decoupled Vector Control Scheme for Dual Three-Phase Permanent Magnet Synchronous Machines," in IEEE Transactions on Industrial Electronics, vol. 61, no. 5, pp. 2185-2196, May 2014.

[20] J. Pyrhonen, J. Tapani, and V. Hrabovcova,` Design of Rotating Electrical Machines. Chichester, U.K.: Wiley, 2008.

[21] R. Wrobel, A. Mlot and P. H. Mellor, "Investigation of end-winding proximity losses in electromagnetic devices," *The XIX International Conference on Electrical Machines - ICEM 2010*, Rome, 2010, pp. 1-6, doi: 10.1109/ICELMACH.2010.5608236.